SPE/IADC Drilling Conference 2017

All manuscripts will be sent through an XML tagging process that will standardize the look of the paper and create links for figures, equations, and references. Figures and tables should be placed directly after the first paragraph they are mentioned in. The XML tagging will not alter the technical content of the paper.

Society of Petroleum Engineers

SPE-184690-MS

The Role of Phosphate Conversion Coatings in Make-up of Casing Connections

D. Ernens, Shell Global Solutions, University of Twente
E. J. van Riet, Shell Global Solutions
M.B. de Rooij, University of Twente
H. R. Pasaribu, Shell Global Solutions
WM. van Haaften, Shell Global Solutions
D. J. Schipper, University of Twente

Abstract

Phosphate conversion coatings are widely used on (premium) casing connections for protection against corrosion. Next to that, in conjunction with the lubricant these coatings provide galling protection. The friction and wear that occurs during make-up and subsequent load cycling determines the sealing performance of the metal-to-metal seal. Therefore, phosphate conversion coatings play an important role in the sealing performance of metal-to-metal seals. An extensive test program was set-up to investigate the role of phosphate coatings during make-up. With pin-on-disc, anvil-on-strip and ring-on-ring tests the interactions between substrate, lubricant and phosphate coating was investigated. A comparison was made between uncoated and coated specimens using base greases, and formulated greases: API modified and two commercially available yellow dopes. The results indicate a strong influence of the phosphate coating leading to damage free make-up, low wear, and less dependence on the lubricant. This is attributed to the formation of a hard and smooth dissimilar surface, the ability to adsorb the lubricant and the generation of a transfer layer on the uncoated counter surface. It is concluded that taking the interaction with phosphates into account could enable lubricants to be tailored for sealing performance and thus can ease the transition to environmentally friendly rated lubricants.

Introduction

Phosphate conversion coatings [1,2] were initially applied on (premium) casing connections for protection against corrosion during storage. A side effect of the presence of the phosphate coatings was improved galling resistance [3]. Phosphate conversion coatings therefore play an important role in proper make-up of casing connections and their subsequent sealing performance.

The premium connection and, for this paper, its metal-to-metal seal should be considered as a (tribo)system [4,5]. It is defined as the combination of lubricant (dope), coating, surface finish and casing material grade under sliding conditions. The contact conditions are determined by the interference of pin and box and the mechanical properties of the pipe material. Next to that, it is important to realize that a connection undergoes sliding in two directions. Make-up (sliding) is predominantly in circumferential direction and micro sliding in axial direction. The micro sliding occurs after make-up because of axial, pressure or thermal load cycling in the well.

The work of [6,7] indirectly assesses the influence of phosphate coatings on the galling behavior of connections during make-up. The coating was applied on the specimens to avoid galling in their screening tests. Implicitly they show that all the fully formulated lubricants show no galling with phosphated surfaces up to extremely high contact stresses. Whereas some of these lubricants normally show galling on bare metal surfaces at very low contact stresses as shown by [7,8].

In general the crystalline phosphate layer provides a chemically incompatible surface with large surface area [1,2]. The large surface area and high surface energy facilitates the adsorption of a lubricant to protect the surface [9–11]. Further, the coating can deform slightly to even out high pressure peaks in the contact and improve conformity of the surfaces [10]. Under sliding conditions the phosphate crystals are crushed and compacted leading to the formation of a hard and smooth glaze layer [12]. Furthermore, due to the properties mentioned it can also serve as a base layer for corrosion inhibitors [13]. In other applications it is used to reduce wear, circumvent galling, and improve running in [14] or as a base layer for paint and organic coatings [9,15].

Sealing performance of contacting elements has been shown to be determined by the surface texture and changes thereof [16,17], the shape distortion [18], the interaction with the lubricant [19] and degradation thereof [16]. A premium connection can for instance be successfully made-up but fail during load cycling because of thermal degradation of the lubricant which led to galling and formation of scratches in the seal area [16]. The initial configuration and subsequent evolution because of friction and wear of the tribosystem is thus important for successful sealing. Moreover the wear should be minimum to stay as close as possible to the intended design contact stresses of the connection manufacturer.

Therefore, it was hypothesized that phosphate conversion coatings play an important role in creating and maintaining an optimal sealing configuration in today’s casing connections. Based on the literature this is not considered as part of connection or lubricant design.

The goal of this paper is to provide understanding of the role of phosphate coatings on casing connections and its contribution to sealing and propose a new direction for connection (tribo) system design. Easing the transition from API modified to yellow dope.

Methods

An extensive test program of three different experiment types was set-up to test this hypothesis. Starting with small scale pin-on-disc tests to simulate the casing connection at the micro level all the way up to a ring-on-ring set-up simulating the metal-to-metal seal of a casing connection.

First, the pin-on-disc tests are designed to investigate make-up sliding by sliding parallel to the machining direction. Next to that, the relatively small stroke length gives insight in the lubricant behavior during micro sliding. The applied contact stresses are equivalent to those in the metal-to-metal seal of a premium connection. The test is used for screening purposes and to gain understanding of the friction and wear properties at the micron scale.

Secondly, the strip test is used for contact stresses and sliding velocities equivalent to those in the connection metal-to-metal seal. The contact is elliptical which is closer to the circumferential [17] line contact in the seal area. The test, however, is limited to unidirectional sliding parallel to the machining direction.

Finally, the ring-on-ring test provides circumferential line contact at equivalent contact stresses and sliding velocities as they occur in metal-to-metal seals. The details will be given in the following sections.

Materials

The pin on disc tests are carried out using an R = 5 [mm] steel (AISI52100) ball against a quenched and tempered steel (AISI4130) disc. The chemical composition is reported in Table 1. The ball is polished and has a surface roughness of S_a = 0.01 [μm] and a surface hardness of 700 HV. The disc is produced by grinding and has a surface roughness of S_a = 0.10 [μm] and a surface hardness of 240 [HV]. See Figure 1 for a measurement of the surface texture. The disc is subsequently zinc or manganese phosphated.

Table 1 Chemical composition used steel grades.

	Chemical composition (%)									
	C	Si	Mn	P	S	Cr	Ni	Cu	Mo	V
API 5CT P110	-	-	-	≤ 0.02	≤ 0.01	-	-	-	-	-
Typical P110	$0.26-0.35$	$0.17-0.37$	$0.40-0.70$	≤ 0.02	≤ 0.01	$0.80-1.10$	≤ 0.20	≤ 0.20	$0.15-0.25$	≤ 0.08
AISI4130	$0.28-0.33$	$0.15-0.35$	$0.40-0.60$	≤ 0.035	≤ 0.04	$0.80-1.10$	-	-	$0.15-0.25$	-
AISI52100	$0.95-1.10$	$0.15-0.30$	≤ 0.25	≤ 0.03	≤ 0.025	$1.30-1.60$	-	-	-	-

The strip tests are done using a steel (P110) anvil against a steel (P110) strip. The anvils and strips are manufactured from a 4" diameter P110 tubing. The chemical composition is reported in Table 1. The anvil is turned and has a surface roughness of S_a=1.6 [μm] and a surface hardness of 320 [HV]. The strip has a lay applied by planing with a cutting element in sliding direction and has a surface roughness of S_a=1.6 [μm] and a surface hardness of 320 [HV]. See Figure 1 for a measurement of the surface textures. These surface properties are common for casing connections. The anvil is subsequently manganese phosphated.

The ring-on-ring tests are performed using steel (P110) “box” against a steel (P110) “pin”. The box is flat, the pin has a round-off radius of 80 [mm]. The box and pin are manufactured from 4" diameter P110 tubing. The chemical composition is reported in Table 1. The box and pin contacting surfaces are manufactured by turning. The surface roughness is S_a =1.6 [μm] and the surface hardness 306 [HV]. The box is subsequently zinc or manganese phosphated.

Note: that in all cases the sliding direction is perpendicular to the paper in Figure 1 or parallel to the machining direction.

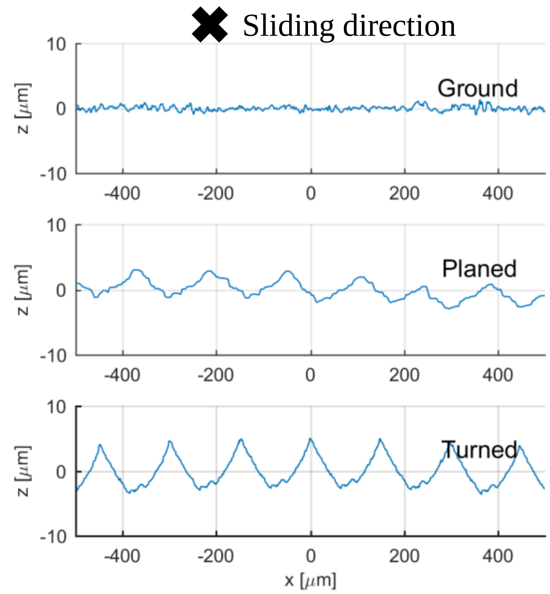

Figure 1 Surface textures of specimens.

Lubricants

To investigate the influence of the separate components of the dope a comparison is made using base oils and base greases versus fully formulated dopes. These are listed in Table 2.

Table 2 Overview of lubricants used in the test program.

Short hand	*Full name*	*Base oil*	*Thickener*	*Additives*
BO	API mod base oil	Mineral based	-	-
Al bg	Aluminium base grease	Mineral based	Aluminium complex	-
Li bg	Lithium base grease	Mineral oil	Lithium complex	-
API mod	API modified	Mineral based	Lithium complex	Lead, copper, zinc, graphite
YD1	Yellow dope 1	Ester oil	Undisclosed	Undisclosed
YD2	Yellow dope 2	Mineral oil	Undisclosed	Undisclosed

Phosphating

After manufacturing, the specimens were cleaned, degreased and water rinsed before they were dipped in the zinc or manganese phosphate bath. The process was carried out under laboratory conditions to ensure maximum uniformity and repeatability for the specimens. See Table 3 for an overview of the process parameters. The resulting coating weights are reported in the final row. Note, however, that because of the morphology a coating thickness is difficult to define [1]. Therefore, weight per unit area is reported in the results.

Table 3 Overview of phosphating steps for the disc and strip specimens.

Step	*Treatment*	*Zinc phosphate (dipping)*	*Manganese phosphate (dipping)*
1	Degreasing	GC 349; 50 g/l; 75°C; 10 min dip time	GC 349; 50 g/l; 75°C; 10 min dip time
2	Rinsing	Cold water	Cold water
3	Activation	GN V6522; 2 g/l; 40°C; 1 min dip time	GN V6563; 4 g/l; 40°C; 1 min dip time
4	Phosphating	GB Z3300, 75°C; 5 min dip time; FA: 18; TAF: 39.8; PP: 57.8; TA: 112; Fe^{++}: 0.9 g/l	GB G4098, 90°C; 5 min dip time 5 g/l GBA H7050; FA: 18.0; TA: 119; Fe^{++}: 1 g/l ;
5	Rinsing	cold water & demineralized water	cold water & demineralized water
6	Drying	oven, 95°C	oven, 95°C
-	Coating weight	4.5 [g/m^2]	10.95 [g/m^2]

SEM micrographs of the coating are shown in Figure 2. Note the difference in magnification. The morphology for the zinc phosphate is the distinct needle shape [1] in agreement with its orthorhombic dipyramidal unit cell. The morphology for manganese phosphate is the characteristic plate structure [1,20] coming from its monoclinic prismatic unit cell. The manganese phosphate process produces a much denser and more refined coating compared to zinc phosphate because of its smaller crystal size [1]. This is also observed here.

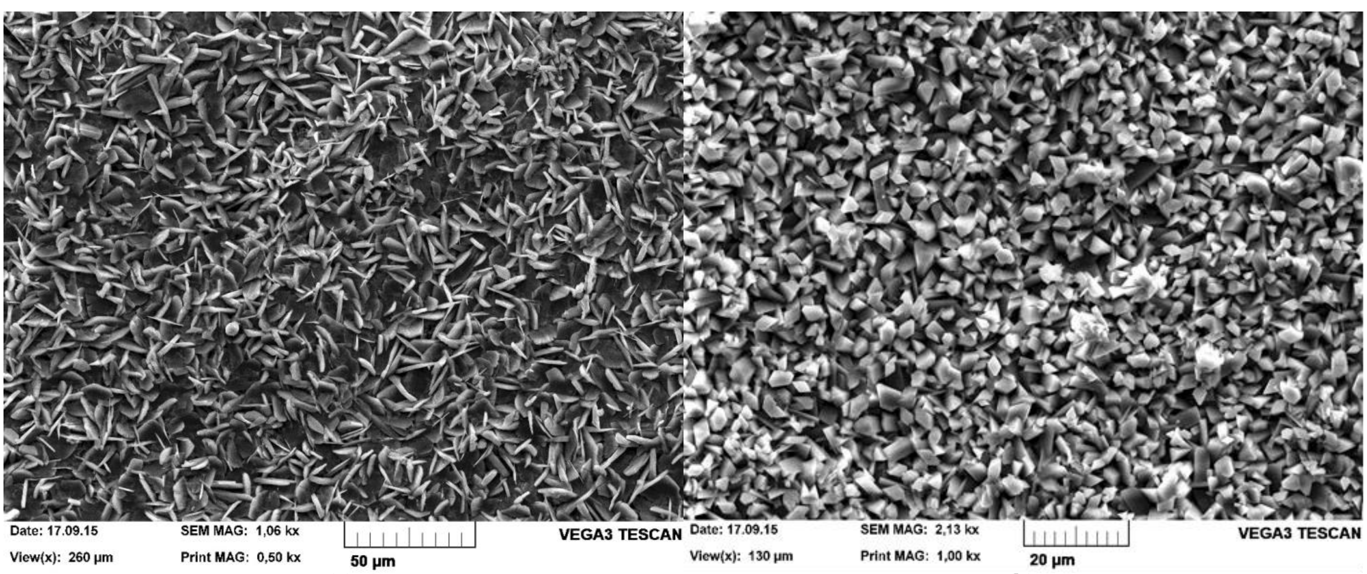

(a) (b)

Figure 2 SEM micrographs of the phosphate crystal sizes. Note the difference in magnification. Figure 2a shows zinc phosphate with is characteristic needle structure. Figure 2b is manganese phosphate with its characteristic plate structure.

Pin on disc

The pin-on-disc experiments are performed with a Bruker UMT-3. The UMT-3 is a modular universal mechanical tester capable of applying a normal load of up to 1000 [N]. The load range and measurement accuracy are determined by the installed load cell. In this case a six degrees of freedom load cell (TFH-50) is installed.

The reciprocating tests are performed at a maximum Hertzian contact stress of 1 [GPa] by applying 10 [N] normal load. The contact spot diameter is approximately 140 [µm] at this stress. The imposed reciprocating sliding length is 500 [µm] at a frequency of 0.5 [Hz]. With 1000 cycles the equivalent sliding length is 1000 [mm]. Both dry and lubricated experiments are executed. Prior to each lubricated experiment the lubricant is applied with a cotton swab on the disc and pin surface. For comparison, a set of reference tests are done on a non-phosphated specimen.

Anvil-on-strip

The strip tests are performed with a Quiri tribometer, see Figure 3 for a schematic of the set-up. In this case, unidirectional sliding tests are performed. The strip is mounted in a tensile tester. On each side of the strip an anvil is pressed at a prescribed load. The strip is then pulled up at a prescribed velocity while measuring the resultant friction force. The sliding tests are performed at a maximum Hertzian contact stress of 1.4 [GPa] by applying 20 [kN] normal load. For the as machined tests, a load ramp is applied over the first 5 strokes. The contact spot is elliptic and approximately 5.7 [mm] x 1.1 [mm]. The sliding velocity is 25 [mm/s]. Up to 50 strokes are made with a sliding length of 31 [mm]. Here also a set of reference tests on bare specimens are performed for comparison.

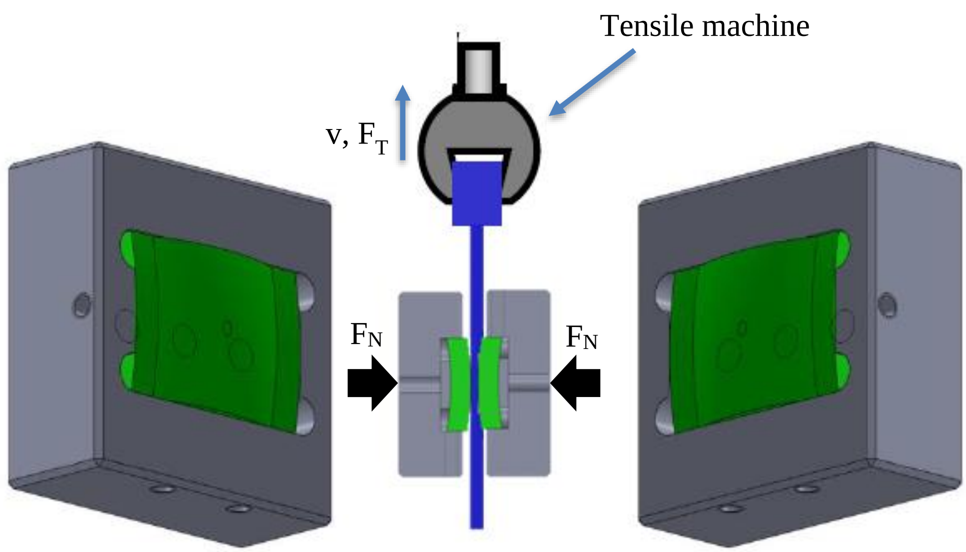

Figure 3 Strip test set-up. The end of the strip is mounted in a tensile machine and a prescribed load is applied on the anvils. The strip is then pulled up under position control leading to a certain friction force.

Ring-on-ring tester

The ring-on-ring tests are performed in an in-house developed test set-up, see Figure 4 for a schematic of the specimen. Sliding tests are performed with continuous contact equivalent to the make-up of a casing connector. The contact configuration of the rings is flat against a round-off of R = 80 [mm] line contact. The contact line diameter is 70 [mm] and the contact width approximately 1 [mm]. The sliding tests are performed at an average maximum Hertzian contact stress of 0.3 [GPa] by applying 30 [kN] normal force. The sliding velocity is 25 [mm/s]. The total sliding length is up to 3 revolutions. At predefined sliding lengths, the specimen is broken apart and a replica of the surface texture is taken to monitor surface evolution. The lubricant is removed and reapplied at each of these steps. Reference tests in as machined versus as machined configuration were performed for comparison.

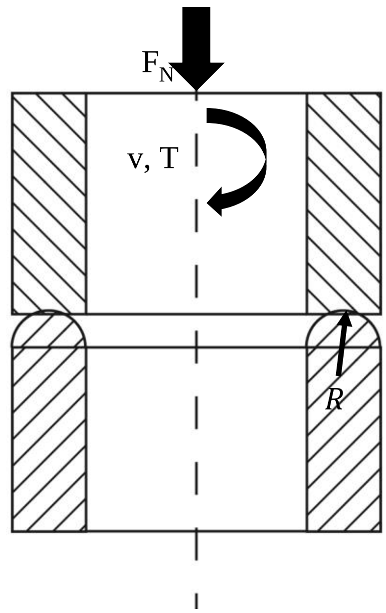

Figure 4 Ring-on-ring schematic. Note the round-off radius R is exaggerated.

Microscopy & metrology

The resulting wear scars are investigated with a Keyence VHX5000 digital light microscope and a Bruker NPFLEX interferometer. Scanning electron microscopy was performed using a Tescan Vega3.

To ensure maximum retention of generated surface layers the specimens are prepared for light microscopy by flushing the grease from the surface with heptane. Final rinsing was done by flushing with acetone and drying to air. For the subsequent measurement of the wear scars with the interferometer the specimens are ultrasonically cleaned in acetone for 5 [min] and wiped dry.

Data processing

The measured reciprocating friction data is processed to get continuous graphs of the coefficient of friction. The locations of the peaks are detected of the absolute values of the measured COF using Matlab® built in `findpeaks`. Next a moving average is taken of the resulting data with a 1[s] window to get smooth trends.

Results and discussion

Pin-on-disc & anvil-on-strip

The reference test results using pin-on-disc are shown in Figure 5. In Figure 5a the processed friction traces are shown. The base greases are not able to protect the surface leading to galling as indicated by the high coefficient of friction. This is confirmed by the resulting wear scar as shown for the lithium base grease in Figure 5b. It is clear that material was pulled out of the surface and transferred to the ball. The transferred material (lump) subsequently created grooves in the disc surface. The failure is typically immediate and results in large surface damage. The friction coefficient does return to a lower value further in the test. This is, however, because the lump finished cutting the groove and widening of the contact lowering the contact stress.

In contrast, the fully formulated greases provided protection either by (metallic) particles and graphite or by forming a reactive tribofilm. This is shown for API modified in Figure 5c. Based on the colors, a combination of zinc, lead and graphite formed a protective film on the surface. Copper does not seem to contribute in lubrication of the sliding contact. This was confirmed using SEM.

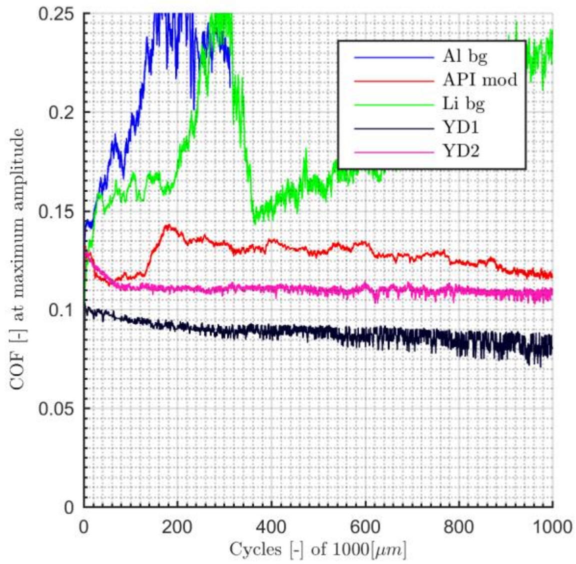

(a)

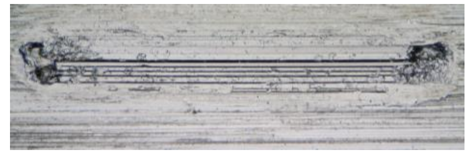

(b)

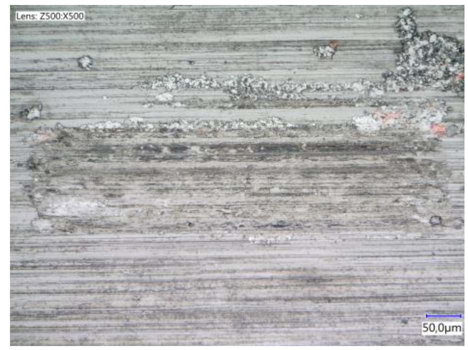

(c)

Figure 5 Reference pin-on-disc experiments in uncoated system. In Figure 5a the friction traces versus cycle are shown for the various lubricants. Figure 5b shows an example of the galling damage after the test with the lithium base grease. Figure 5c shows the result of a test with API modified.

The reference tests results using the strip test set-up are shown in Figure 6. Under the harsher test conditions all lubricants fail in galling as indicated by the high initial friction coefficient in Figure 6a. The lubricants that failed in pin-on-disc perform also the worst in the strip test. In all cases the failure was initiated because the lubricants cannot build up the protective film that was found in the pin-on-disc test which results in adhesive wear leading to galling [21].

Two of those failed specimens are shown in Figure 6b for Li bg and Figure 6c for API mod. The results were close to identical on each side. Therefore, the wear scars of anvil and strip are shown for one side of the strip. In each case galling was severe, however, the Li bg shows the largest surface damage with big chunks of material being removed. API modified is more well behaved only showing deep scratching of the surface. Again the friction coefficient goes down with subsequent strokes because of widening of the contact lowering the contact stress.

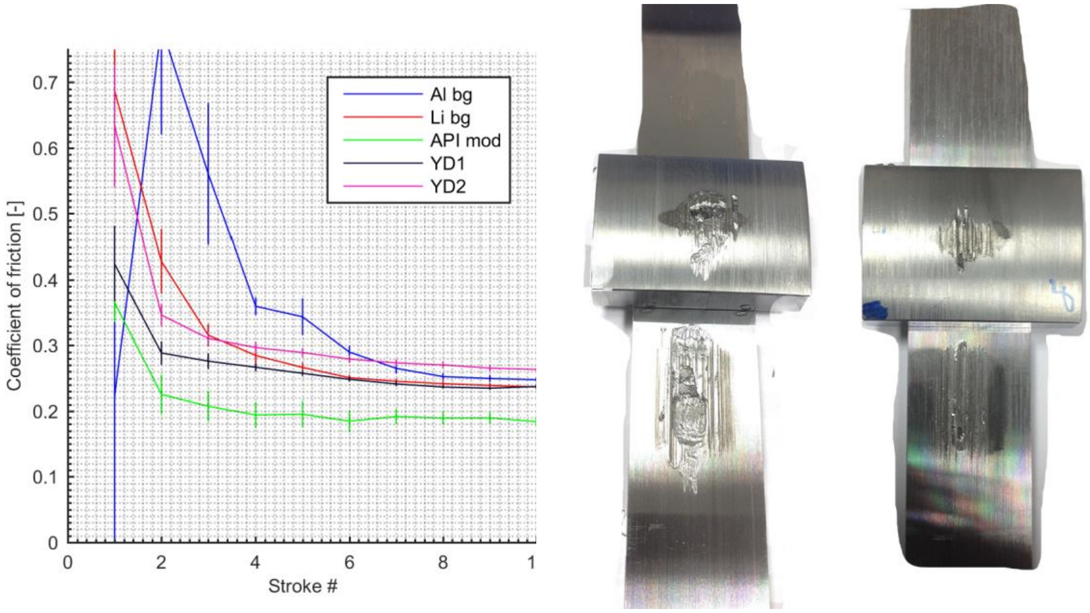

(a) (b) (c)

Figure 6 Reference strip test experiments in uncoated system. In Figure 6a the friction traces versus stroke are shown for the various lubricants. Figure 6b shows a macrograph of a galled Li bg specimen. Figure 6c shows a macrograph of the galled API mod specimen.

For easy comparison and brevity, the results above will be summarized using the maximum friction coefficient, observations from light microscopy and interferometry, and scanning electron microscopy hereafter.

The summary for the pin-on-disc and strip tests are shown in Figure 7. For clarity, a coefficient of friction of 1 indicates galling based on the combination of the friction trace and observations of the wear scar. Figure 7a shows the summary of the friction traces as shown in Figure 5a including the zinc and manganese phosphate results. As discussed the base greases fail by galling and the full formulation greases give acceptable friction and wear results.

When changing to a zinc or manganese phosphate disc the earlier failing lubricants show low friction and wear behaviour. Even the base oil that is used to formulate the aluminium base grease produces acceptable results. Furthermore, the coefficient of friction is not varying a lot between the different lubricants.

The same set of lubricants was tested using the strip tester. Here a higher contact stress is combined with a higher sliding velocity. The results are summarized in Figure 7b. As discussed (Figure 6), in the uncoated tests all lubricants fail in galling which is attributed to the more realistic test conditions. In all cases failure is immediate, the first stroke will directly indicate the galling resistance. This is in line with the observations of previous investigators [3,7,8] as discussed in the introduction.

As before, coating one of the surfaces (anvil here) with manganese phosphate changes the behavior drastically. Now all lubricants protect the surface in conjunction with the manganese phosphate coating. No galling was observed. As in the pin-on-disc tests, the maximum coefficient of friction is approximately the same for all tests which indicates that the sliding behavior is dominated by the base oil and the manganese phosphate coating. Next to that, comparing pin-on-disc with anvil-on-strip the trends in maximum COF are the same.

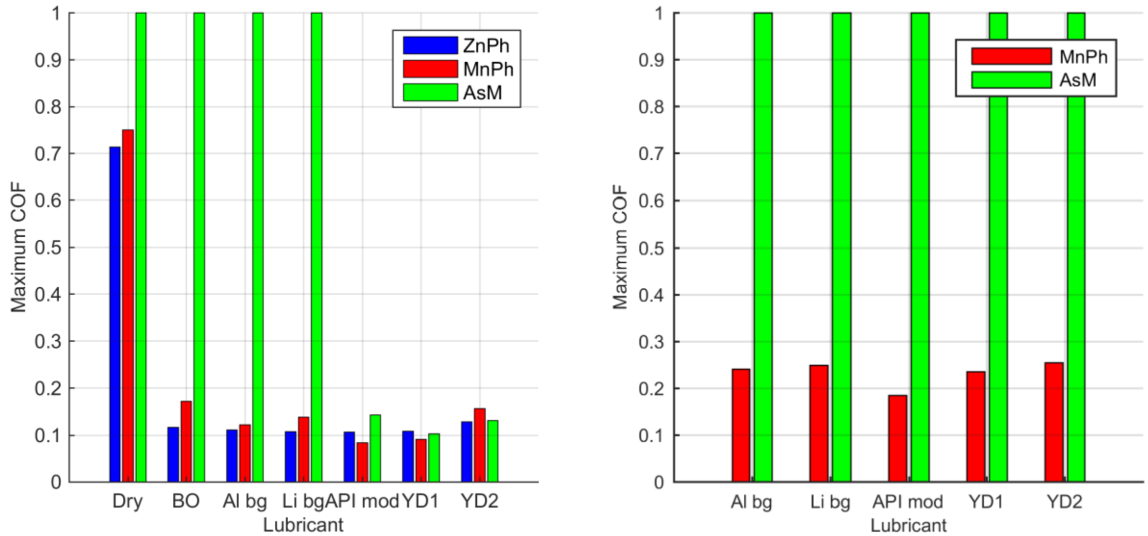

(a) (b)

Figure 7 Summarized results for pin-on-disc and strip tests. Figure 7a shows the results of the pin-on-disc tests for as machined, and zinc and phosphated discs. Note that a COF of 1 indicates galling. Figure 7b shows the results of the striptests for as machined and manganese phosphated anvils.

Ring-on-ring

The results of the ring-on-ring tests cannot be satisfactorily captured in a friction trace. Typically (onset of) galling is not detected in the torque signal because of the localized nature versus the relatively large surface area of the specimen. Therefore, only the surface damage or lack thereof is assessed.

The outcome of the reference test for the ring-on-ring set-up is shown in Figure 8. The specimen was made-up with API modified. Large areas of surface damage are visible due to galling particularly in the region marked by C. Note that the observation is made after one revolution. Even though a substantial area was galling, the onset was not observed on the torque measurements. This shows the inability of detecting (onset of) galling during full connection (including threads) make-up based on only the torque-turn graph.

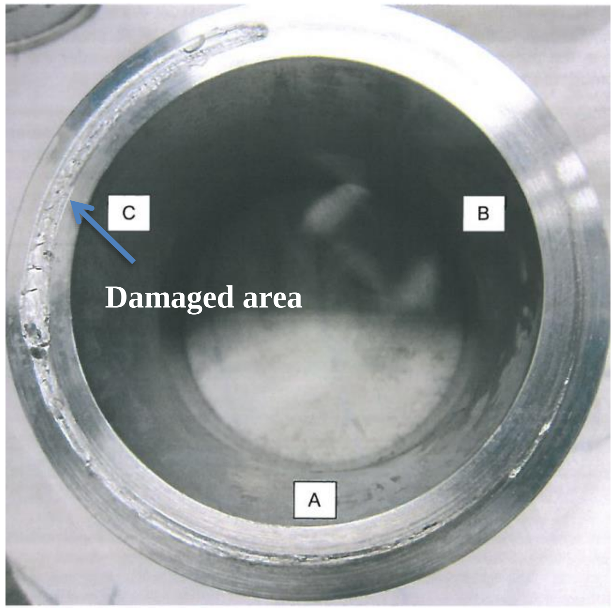

Figure 8 Results of the as machined reference test. Surface damage after make-up sliding with API modified. Letters indicate orientation of specimen to match with the counter surface.

In Figure 9 the results are shown after make-up sliding with zinc phosphate specimens (Figure 9a/b) and manganese phosphate specimens (Figure 9c/d) against as machined pins. The conditions were the same as for the specimen in Figure 8. The surfaces are burnished and show no signs of surface damage or galling. On the phosphated box specimens a smooth and flat glaze layer is formed in the sliding contact. On the as machined pin specimens transfer of material can be observed.

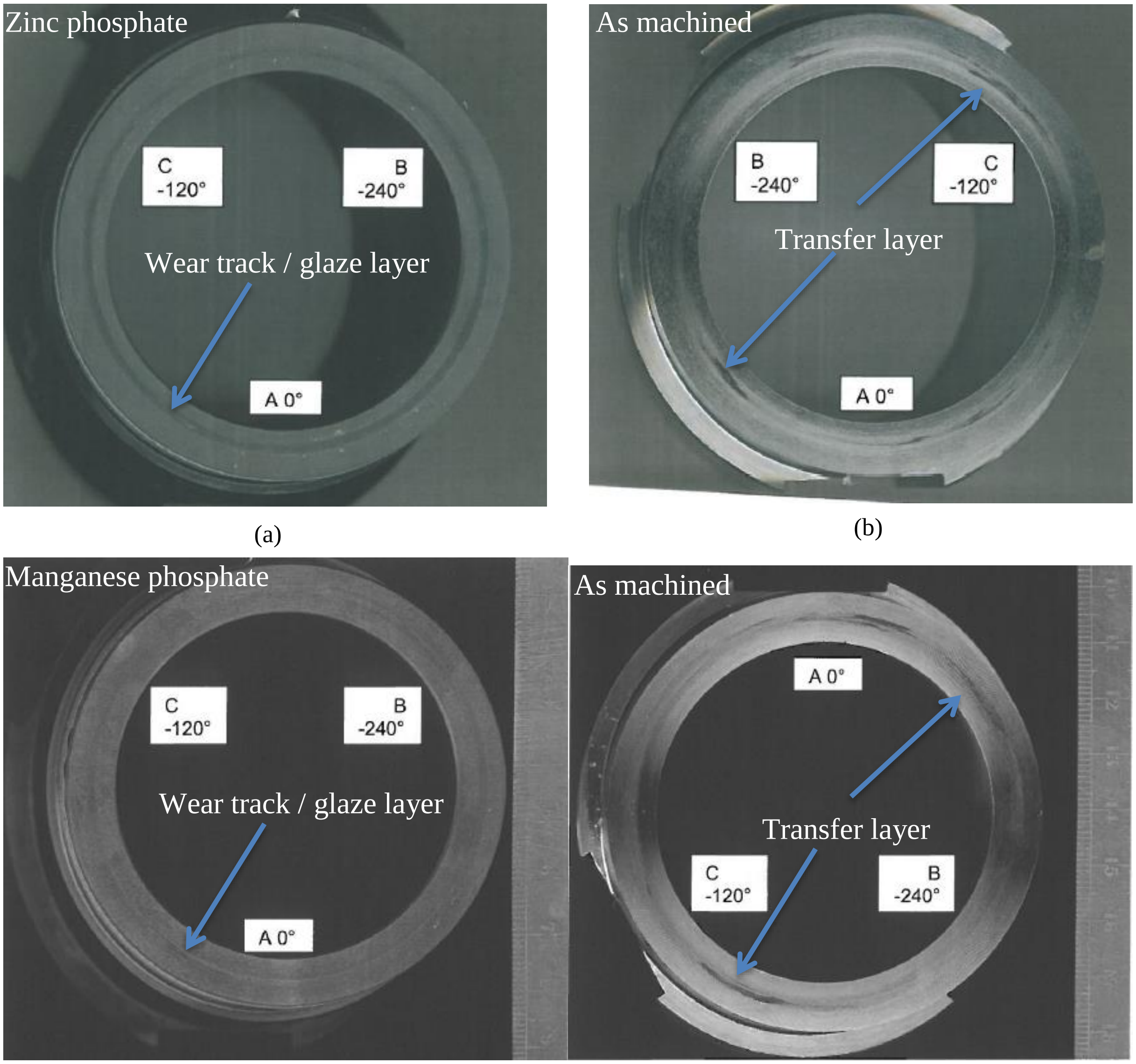

(a) (b)

(c) (d)

Figure 9 Surface after make-up sliding with phosphate specimens lubricated by API modified. Letters indicate orientation of specimen to match with the counter surface. Figure 9a and Figure 9b show the result of a zinc phosphate box against an as machined pin. Figure 9c and Figure 9d show the results of a manganese box against an as machined pin. Sliding conditions were the same. No galling is observed.

The profiles of the surfaces in Figure 9 after running are shown in Figure 10. The pin profiles need to be compared to the initial profiles in Figure 1. In both cases it is clear that minimal wear has occurred on the pin side. This keeps the contact situation close to the as designed contact stresses increasing the likelihood of sealing if this were a metal-to-metal seal.

Zinc Phosphate Figure 9a/b

Manganese Phosphate Figure 9c/d

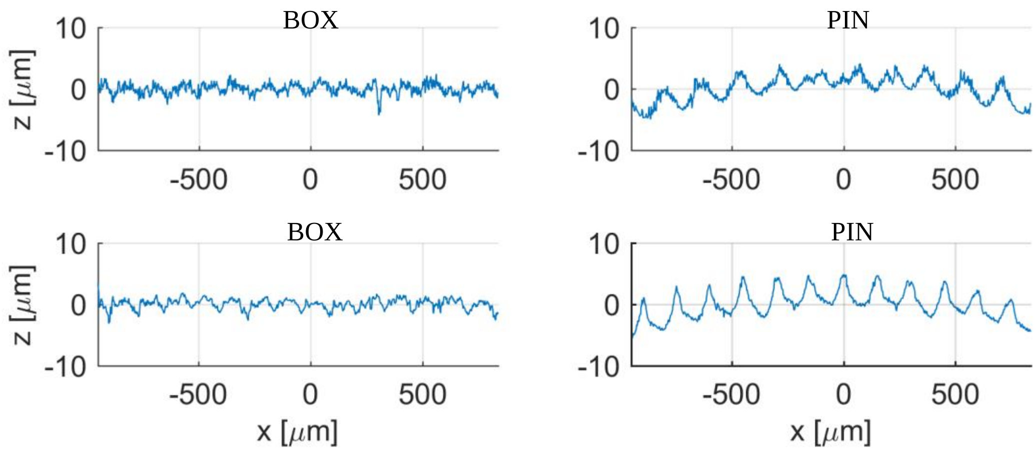

Figure 10 Surface profiles of ring-on-ring specimens after make-up sliding with API modified.

Combining the observations from pin-on-disc, anvil-on-strip, and ring-on-ring the following can be deducted. Phosphate conversion coatings play a critical role in damage free make-up and subsequent micro sliding of a casing connection. In all tests the phosphate coating reduces the likelihood of galling significantly, regardless of the lubricant. Based on the observations in the tests the reason for this is threefold:

1. A smooth hard flat [12] dissimilar surface [1] against a rough surface minimizes adhesion and thus wear and most importantly galling.
2. The phosphate provides a reservoir for the lubricant which replenishes the contact [1].
3. Generation of a tribolayer on the bare steel counter surface adding an additional barrier to prevent galling.

As discussed in the introduction, make-up sliding determines the initial sealing configuration and thus performance. It is therefore speculated that the likelihood of sealing is increased by the presence of these galling preventing mechanisms.

Conclusions

The role of phosphate coatings on casing connections was investigated using pin-on-disc anvil-on-strip, and ring-on-ring tests. From the results in this paper it is clear that this role is crucial for reliable performance of casing connections. This has been recognized by the industry judging by the extensive use of phosphating on casing connections. The results outlined in this paper should give this scientific support.

The results indicate the following role for the phosphate coatings:

1. The phosphate coating provides a dissimilar and large area surface. The benefit was shown to be twofold. The dissimilar nature compared to the steel counter surface ensures no adhesion. The large surface area lets the coating be an adsorbent for the oil and the particles.
2. The originally rough phosphate coating is formed into a smooth glaze layer under make-up sliding as shown in small scale tests. It is speculated that this yields an ideal configuration for sealing.
3. The phosphate coating provides a pre-applied tribolayer protecting the surface from the onset. The results show that the dependence on the lubricant for galling prevention is removed.

The conclusion opens the door for lubricants that are tailored for sealing performance by taking advantage of the presence of a phosphate coating. Furthermore, it can ease the transition to environmentally friendly rated lubricants. This will be the subject of future work.

Acknowledgements

We would like to thank Shell Global Solutions for giving us the opportunity to publish our work and Chemetall GmbH for sharing their expertise on phosphate coatings.

References

[1] Rausch, W., 1990, The phosphating of metals, ASM International.

[2] Narayanan, T. S. N. S., 2005, "Surface pretreatment by phosphate conversion coatings - A review," Reviews on Advanced Materials Science, **9**(2), pp. 130–177.

[3] Ertas, A., 1992, "Experimental Investigation of Galling Resistance in OCTG Connections," Journal of Manufacturing Science and Engineering, **114**(1), p. 100.

[4] Salomon, G., 1974, "Application of Systems Thinking to Tribology," A S L E Transactions, **17**(4), pp. 295–299.

[5] Czichos, H., and Winer, W. O., 1978, Tribology: A Systems Approach to the Science and Technology of Friction, Lubrication and Wear (Tribology Series, 1), Elsevier.

[6] Ertas, A., Cuvalci, O., and Carper, H. J., 1999, "Determination of Friction Characteristics of J-55 OCTG Connections Lubricated with Environmentally Safe Thread Compound," Tribology Transactions, **42**(4), pp. 881–887.

[7] Carper, H. J., Ertas, A., Issa, J., and Cuvalci, O., 1992, "Effect of Some Material, Manufacturing, and Operating Variables on the Friction Coefficient in OCTG Connections," Journal of Tribology, **114**(4), p. 698.

[8] Carper, H. J., Ertas, A., and Cuvalci, O., 1995, "Rating Thread Compounds for Galling Resistance," Journal of Tribology, **117**(4), p. 639.

[9] Burke, D., 2005, "The Sliding Friction of Bonded Solid Lubricants," University of central Lancashire.

[10] Khaleghi, M., Gabe, D. R., and Richardson, M. O. W., 1979, "Characteristics of manganese phosphate coatings for wear- resistance applications," Wear, **55**(2), pp. 277–287.

[11] Weng, D., Jokiel, P., Uebleis, A., and Boehni, H., 1997, "Corrosion and protection characteristics of zinc and manganese phosphate coatings," Surface and Coatings Technology, **88**(1-3), pp. 147–156.

[12] Ernens, D., de Rooij, M. B., Schipper, D. J., Pasaribu, H. R., Riet, E. J. Van, and Haaften, W. M. Van, 2017, "Mechanical Characterization and Single Asperity Scratch Behaviour of Dry Zinc and Manganese Phosphate Coatings," Tribology International.

[13] Totik, Y., 2006, "The corrosion behaviour of manganese phosphate coatings applied to AISI 4140 steel subjected to different heat treatments," Surface and Coatings Technology, **200**(8), pp. 2711–2717.

[14] Westberg, H. J., Nilsson, P. H., Rosén, B.-G., and Stenbom, B., 2000, "Manganese Phosphating of Gears and Surface Roughness Consequence," Proceedings of the 26th Leeds-Lyon Symposium on Tribology, pp. 145–153.

[15] Pokorny, P., Szelag, P., Novak, M., Mastny, L., and Brozek, V., 2015, "Thermal stability of phosphate coatings on steel," Metalurgija, **54**(3), pp. 489–492.

[16] Inose, K., Sugino, M., and Goto, K., 2016, "Influence of Grease on High-Pressure Gas Tightness by Metal-to-Metal Seals of Premium Threaded Connections," Tribology Online, **11**(2), pp. 227–234.

[17] Pérez-Ràfols, F., Larsson, R., and Almqvist, A., 2016, "Modelling of leakage on metal-to-metal seals," Tribology International, **94**, pp. 421–427.

[18] Ledoux, Y., Lasseux, D., Favreliere, H., Samper, S., and Grandjean, J., 2011, "On the dependence of static flat seal efficiency to surface defects," International Journal of Pressure Vessels and Piping, **88**(11-12), pp. 518–529.

[19] Murtagian, G. R., Fanelli, V., Villasante, J. A., Johnson, D. H., and Ernst, H. A., 2004, "Sealability of Stationary Metal-to-Metal Seals," Journal of Tribology, **126**(3), p. 591.
[20] Moore, P. B., and Araki, T., 1973, "Hureaulite, MN52+ (H2O) 4 [PO3 (OH)] 2 [PO4] 2 - Its Atomic Arrangement," American Mineralogist, **58**(3-4), pp. 302–307.
[21] Stachowiak, G., and Batchelor, A. W., 2013, Engineering Tribology, Butterworth-Heinemann.